

## THE MID-INFRARED EMITTING DUST AROUND AB AUR

C. H. CHEN &amp; M. JURA

Department of Physics and Astronomy, University of California, Los Angeles, CA 90095-1562;  
cchen@astro.ucla.edu; jura@astro.ucla.edu*Draft version November 19, 2018*

## ABSTRACT

Using the Keck I telescope, we have obtained 11.7  $\mu\text{m}$  and 18.7  $\mu\text{m}$  images of the circumstellar dust emission from AB Aur, a Herbig Ae star. We find that AB Aur is probably resolved at 18.7  $\mu\text{m}$  with an angular diameter of 1.2'' at a surface brightness of 3.5 Jy arcsec<sup>-2</sup>. Most of the dust mass detected at millimeter wavelengths does not contribute to the 18.7  $\mu\text{m}$  emission, which is plausibly explained if the system possesses a relatively cold, massive disk. We find that models with an optically thick, geometrically thin disk, surrounded by an optically thin spherical envelope fit the data somewhat better than flared disk models.

*Subject headings:* stars: individual (AB Aur)— circumstellar matter— planetary systems: formation

## 1. INTRODUCTION

Herbig Ae/Be stars are pre-main sequence progenitors of intermediate mass A- and B-type stars which possess strong infrared excesses, dominated by thermal emission from dust grains. It is generally thought that these stars possess circumstellar disks (Mannings & Sargent 1997, 2001) in which planets might form. The grain properties (size, temperature and composition) and the macroscopic geometry of the mid-infrared emitting dust around these stars are not yet well determined. In the simplest models, Herbig Ae/Be stars possess optically thick, geometrically thin disks which produce spectral energy distributions (SEDs) with  $\nu F_\nu \propto \nu^{4/3}$ , steeper than the observed SEDs (Hillenbrand et al. 1992). Several groups have suggested a variety of explanations for this discrepancy such as flared disks with a surface layer of small grains (Chiang & Goldreich 1997) and geometrically thin disk embedded in spherically symmetric envelopes (Miroshnichenko et al. 1999). We have carried out a high resolution mid-infrared imaging study of AB Aur to learn about the spatial distribution of warm dust which may allow us to distinguish among models.

AB Aur is a A0 Ve+sh (shell) Herbig Ae star with a *Hipparcos* distance of 144 pc from the Sun. Since AB Aur lies near the zero age main sequence, there is some uncertainty in estimating its age. Mannings & Sargent (1997) estimate a total stellar luminosity and effective temperature,  $L_* = 53.6 L_\odot$  and  $T_{eff} = 10210K$ , which corresponds to a stellar age and mass of  $\sim 3\text{-}5$  Myr and  $2.5 M_\odot$ , using pre-main sequence tracks computed by D'Antona & Mazzitelli (1994). Van den Ancker, de Winter, & Tjin A Djie (1998) have estimated a total stellar luminosity and effective temperature,  $L_* = 47 L_\odot$  and  $T_{eff} = 9500K$ , which corresponds to a stellar age and mass of  $\sim 2$  Myr and  $2.4 M_\odot$ , using pre-main sequence tracks computed by Palla & Stahler (1993). AB Aur is an excellent source for high resolution mid-infrared imaging because it is bright and close by. It is one of four stars in the Hillenbrand et al. (1992) sample which possess a *Q* band magnitude brighter than -1.0 and lies at a distance less than 150 pc. All models for the dust distribution around AB Aur presume that it is a single star. If AB Aur is a binary, then

current models are incomplete.

Millimeter aperture synthesis imaging of AB Aur has resolved a rotating disk of <sup>13</sup>CO (*J*=1→0), with a radius of  $\sim 450$  AU and at a position angle of 79°, around AB Aur, with velocities consistent with Keplerian rotation (Mannings & Sargent 1997). Based upon the aspect ratio of the major:minor axes, Mannings & Sargent (1997) find an inclination of 76° for the disk. Previous mid-infrared imaging studies of AB Aur report spatially resolved observations of the mid-infrared emission at 17.9  $\mu\text{m}$  using the 5 m Hale telescope (Marsh et al. 1995). They find an elongated disk, with an East-West extent of 80±20 AU and a North-South extent of 25±20 AU and thus a position angle consistent with that observed for the CO disk. However, subsequent higher resolution near infrared interferometry (Millan-Gabet et al. 1999; Millan-Gabet, Schlorerb, & Traub 2001) and scattered light imaging of AB Aur (Grady et al. 1999) suggest a disk inclination of less than 45°.

The dust around AB Aur has been studied with a variety of techniques. Near infrared, interferometric observations at *H* and *K'* bands have resolved a ring of emission with a radius of 0.35 AU (Millan-Gabet et al. 1999). *ISO* 2-200  $\mu\text{m}$  spectra have revealed the presence of PAH, FeO, and olivine emission features and Si-O and O-Si-O bending modes (van den Ancker et al. 2000). However, to date, no complete view of the dust around AB Aur has been constructed. Thus, we discuss models for the dust around AB Aur in the context of millimeter continuum fluxes, infrared spectra, and near infrared visibilities. In addition, we compare models for the dust around AB Aur with our high resolution Keck 18.7  $\mu\text{m}$  map.

## 2. OBSERVATIONS

Our data were obtained on 2000 February 20 (UT) and 2000 August 9 (UT) at the Keck I telescope using the Long Wavelength Spectrometer (LWS) which was built by a team led by B. Jones and is described on the Keck web page. The LWS is a 128×128 SiAs BIB array with a pixel scale at the Keck telescope of 0.08'' and a total field of view of 10.2''×10.2''. We used the “chop-nod” mode of observing and two different filters: 11.2-12.2  $\mu\text{m}$  and 18.2-19.2  $\mu\text{m}$ . The seeing on 2000 August 9 was significantly better

than that on 2000 February 20; thus, we concentrate our analysis on the data obtained in August 2000. We used  $\alpha$  Cet for flux and point spread function (PSF) calibrations and MWC 480 (an unresolved Herbig Ae star) and  $\gamma$  And for additional PSF calibrations. The data were reduced at UCLA using standard LWS routines.

We flux calibrate our February and August data using the result for  $\alpha$  Tau and  $\alpha$  Cet that  $F_\nu(11.5\mu\text{m}) = 507.8$  Jy and 174.5 Jy, respectively and  $F_\nu(19.3\mu\text{m}) = 189.4$  Jy and 66.3 Jy (Gezari et al. 1987) extrapolated to our bands assuming that  $F_\nu \propto \nu^2$  between 10 and 20  $\mu\text{m}$ . For AB Aur, we find  $F_\nu(11.7\mu\text{m}) = 25 \pm 2$  Jy and  $19 \pm 2$  Jy for February and August, respectively, and  $F_\nu(18.7\mu\text{m}) = 31 \pm 2$  Jy and  $17 \pm 2$  Jy for February and August, respectively. We conservatively estimate the uncertainties associated with our measurements from the drift in the fluxes of all of our standard stars throughout the night. Comparison of our fluxes and of published fluxes in the 10  $\mu\text{m}$  and 20  $\mu\text{m}$  bands (listed in Tables 2 and 3) suggest that AB Aur is variable at mid-infrared wavelengths. The  $24 \pm 10\%$  11.7  $\mu\text{m}$  variability we observe is consistent with the  $21.7 \pm 6.6\%$  IRAS 12  $\mu\text{m}$  6 month variability reported by Prusti & Mitsukevich (1994). The  $46 \pm 8\%$  18.7  $\mu\text{m}$  variability we observe is significantly larger than the  $14.3 \pm 8.5\%$  variability IRAS 25  $\mu\text{m}$  6 month variability reported by Prusti & Mitsukevich (1994). However, the absolute magnitudes of our 18.7  $\mu\text{m}$  fluxes are similar to 17  $\mu\text{m}$  fluxes measured using *ISO* and the IRTF, 24.4 Jy (Thi et al. 2001) and 22.7 Jy (Richter et al. 2002) respectively.

The color temperature, inferred from our 11.7  $\mu\text{m}$  and 18.7  $\mu\text{m}$  photometry, for our data agrees within the error bars for our two epochs of observations. The flux ratio,  $F_\nu(11.7\mu\text{m})/F_\nu(18.7\mu\text{m})$ , is  $0.8 \pm 0.1$  and  $1.1 \pm 0.2$  for February 2000 and August 2000, respectively. Thus, we can not rule out the possibility that changes in intrinsic luminosity of the star generate the observed variability. AB Aur possesses strong variability in the H $\alpha$  P Cygni profile and in measurements of the linear polarization of UBVR. Based upon monitoring of these diagnostics in 1993 and 1994, Beskrovnaya et al. (1995) suggest that circumstellar inhomogeneities may be responsible for the variability on hour to month long timescales. Prusti & Mitsukevich (1994) suggest that dust formation in the stellar wind or dust on eccentric orbits may be responsible for the mid-infrared variability.

We generate images from our chop-nod sets by coadding chop pairs from both nod positions in each of our nod sets. The 18.7  $\mu\text{m}$  PSF contains a ghost and diffuse asymmetric scattering while the 11.7  $\mu\text{m}$  PSF is clean. Although the seeing was excellent, the PSFs varied somewhat during the night. We show line cuts through AB Aur and our 11.7  $\mu\text{m}$  standards in Figure 1a and through AB Aur and our 18.7  $\mu\text{m}$  standards perpendicular to and parallel to the scattered light in Figures 1b and 1c. The Airy rings can be seen in all of the 18.7  $\mu\text{m}$  line cuts and half of the 11.7  $\mu\text{m}$  line cuts. Since there is some variation in the PSF at 18.7  $\mu\text{m}$ , we compare our images of AB Aur to 3 PSF calibrators:  $\alpha$  Cet, observed 57 minutes earlier, MWC 480 (an unresolved Herbig Ae star), observed 11 minutes later, and  $\gamma$  And, observed 2 hours, 26 minutes earlier than AB Aur. We use MWC 480 as our primary PSF because it was observed closest in time to AB Aur. We also use  $\gamma$

And because it was observed with the worst seeing during the evening.

AB Aur is probably resolved at 18.7  $\mu\text{m}$  with an angular diameter of 1.2'' at a surface brightness of 3.5 Jy arcsec<sup>-2</sup> (10% of the maximum surface brightness). An image of our calibrator  $\alpha$  Cet at 18.7  $\mu\text{m}$  is shown in Figure 2 with contours showing 1%, 2%, 3%, 5%, 10%, 25%, 50%, and 99% of the maximum surface brightness. We display  $\alpha$  Cet instead of MWC 480 because it is a significantly bright object, making the ghost and diffuse scattered light significantly easier to see. An image of AB Aur at 18.7  $\mu\text{m}$  is shown in Figure 3 for comparison with the same contours as in the image of  $\alpha$  Cet. The diameter of AB Aur at 10% of the maximum surface brightness is 50% larger than the same contour in the image of  $\alpha$  Cet. In addition, the lowest surface brightness contours (1%, 2%, 3%, and 5%) are more symmetric in the image of AB Aur than in the image of  $\alpha$  Cet. Our image of AB Aur at 18.7  $\mu\text{m}$  does not exhibit the same asymmetry reported by Marsh et al. (1995) at 17.9  $\mu\text{m}$ . AB Aur appears unresolved at 11.7  $\mu\text{m}$ , with a Full Width at Half Maximum (FWHM) of 0.30'', consistent with a point source.

### 3. THE CIRCUMSTELLAR DISK AND MORE?

The total mass of dust around AB Aur has been estimated from millimeter continuum measurements in an elliptical beam with FWHM  $3.5'' \times 5.6''$ . At  $\lambda = 2.7$  mm, Mannings & Sargent (1997) find that AB Aur appears unresolved and measured a flux,  $F_\nu(2.7\text{ mm}) = 10.6 \pm 0.4$  mJy which, in their models, corresponds to  $M_{dust} = 2.0 \times 10^{29}$  g.

We can estimate the minimum mass of warm dust contributing to the 18.7  $\mu\text{m}$  flux. If the dust is optically thin and the population has a single temperature, then

$$M_{warm} = \frac{F_\nu D_*^2}{B_\nu(T_{gr}) \chi_\nu} \quad (1)$$

(Jura et al. 1995) where  $\chi_\nu$  is the dust absorption opacity and  $D_*$  is the distance to the object. We estimate the temperature of the dust,  $T_{gr}$ , from the ratio of our 11.7  $\mu\text{m}$  and 18.7  $\mu\text{m}$  fluxes, assuming a single population of grains. If  $T_{gr} = 250$  K,  $F_\nu(18.7\mu\text{m}) = 17.2$  Jy, and  $\chi_\nu = 1000$  cm<sup>2</sup>/g (Ossenkopf, Henning, & Mathis 1992), then  $M_{warm} = 1.2 \times 10^{25}$  g, substantially less than that inferred from millimeter continuum measurements. Therefore, a large amount of cold dust must exist in the system, presumably in a disk.

### 4. COMPARISON WITH MODELS

We use our data to evaluate the following four detailed models for the dust around AB Aur: (1) An optically thick, geometrically thin disk surrounded by an optically thin, spherically symmetric envelope (Vinkovic et al. 2002). (2) Two spherically symmetric dust shells, whose grain properties (composition, size and spatial distribution) are inferred from *ISO* 2 - 200  $\mu\text{m}$  spectra (Bouwman et al. 2000). (3) A geometrically thin, flared disk in vertical hydrostatic equilibrium (D'Alessio et al. 1998). (4) A flared disk with an optically thin surface layer of small grains and an infrared emitting rim (Dullemond, Domink, & Natta 2001).

We convolve these models for the predicted surface brightness of AB Aur at  $18.7 \mu\text{m}$  with the PSF and compare them with our observations of AB Aur. Each model was interpolated to provide surface brightnesses on the same grid as the observations. Since line cuts through each of the models, convolved with a PSF, compared with the AB Aur data look similar independent of position angle, we only show line cuts along the North-South direction of each of the models, convolved with a PSF, compared with the AB Aur data. In Figure 4a, MWC 480, an unresolved Herbig Ae star observed closest in time to AB Aur, was used as the PSF. In Figure 4b,  $\gamma$  And, the most extended PSF observed during the night, was used. Line cuts through different position angles appear similar; thus, we show line cuts through only one orientation. In addition, we calculate the reduced  $\chi^2$  for the inner  $1.2'' \times 1.2''$  centered on AB Aur, using MWC 480 as the PSF. In both analyses, we scale the image of the model, convolved with the PSF, so that the maximum surface brightness is equal to the measured maximum surface brightness of AB Aur. Since AB Aur is located at a distance of 144 pc, the flux expected from the stellar photosphere at  $18.7 \mu\text{m}$ ,  $F_\nu(18.7\mu\text{m}) = 0.032$  Jy, is significantly less than the smallest measured excess flux,  $F_\nu(18.7\mu\text{m}) = 17.2$  Jy, and can be neglected. We calculate the reduced  $\chi^2$  for each model assuming that the uncertainty in the surface brightness is 10%, approximately the uncertainty in the  $18.7 \mu\text{m}$  photometry. Finally, we also compare the models to measured near infrared interferometric visibilities, infrared spectra, and millimeter continuum measurements.

#### 4.1. A Spherically Symmetric Envelope?

Vinkovic et al. (2002) have modeled the SED of AB Aur with a system which consists of a star with radius,  $R_*$ , and effective temperature,  $T_*$ , surrounded by a geometrically thin and optically thick passive disk extending from  $R_*$  to an outer radius  $R_{disk} = 240$  AU. The optically thick disk is assumed to have an inclination,  $i = 76^\circ$ , consistent with the CO observations of Mannings & Sargent (1997). They also incorporate a spherical dust envelope with an inner radius,  $R_{sub} = 99.3 R_*$  and an outer radius,  $1000 R_{sub}$ . At distances less than  $R_{sub}$ , grains in the envelope are sublimated. The mass density and grain size distributions are given by

$$\rho(r) = \rho_o \left[ \left( \frac{R_{sub}}{r} \right)^2 + \frac{0.2R_{sub}}{r} \right] \quad (2)$$

$$n(a) = Aa^{-3.5} \quad (3)$$

where  $r$  is the distance between the star and the circumstellar material and  $a$  is the grain radius. The dust grains are assumed to be an interstellar mixture of 53% silicates and 47% graphite by number (Draine & Lee 1984) with a minimum grain radius,  $a_{min} = 0.005 \mu\text{m}$ , and a maximum grain radius  $a_{max} = 0.250 \mu\text{m}$ . They assume an optically thick, geometrically thin (flat) disk with an outer temperature of 25 K, a disk mass,  $M_{disk} = 8.6 \times 10^{30}$  g, and an envelope mass,  $M_{env} = 2.8 \times 10^{27}$  g, corresponding to an optical depth,  $\tau_V = 0.44$ , consistent with the value measured by van den Ancker et al. (2000) ( $A_V = 0.5$ ). Their best fit model for the SED for AB Aur yields a total flux  $F_\nu(18.7\mu\text{m}) = 25$  Jy with 12 Jy from the disk and 13 Jy from the envelope.

We compare the inner  $1.2'' \times 1.2''$  of our  $18.7 \mu\text{m}$  map of AB Aur with the model (Vinkovic et al. 2002). When the intensity map for this model is convolved with the PSF and scaled so that the maximum surface brightness is equal to that measured for AB Aur, the reduced  $\chi^2 = 4.6$ . Their model agrees well with our data.

However, the Vinkovic et al. (2002) model does have some limitations. They do not provide a physical explanation for the stability of the envelope. In addition, their model does not attempt to reproduce the detailed infrared spectra; a standard interstellar grain mixture is assumed. While the near infrared fluxes are fit, the measured visibilities are not considered. Finally, the model assumes a dust disk mass which is more than an order of magnitude higher than is inferred from millimeter continuum measurements.

#### 4.2. Modeling the Infrared Spectra

Bouwman et al. (2000) infer dust composition, spatial distribution, and grain sizes by fitting *ISO* 2 - 200  $\mu\text{m}$  spectra. For simplicity, they assume that the dust around AB Aur is optically thin and contained within spherically symmetric shells and neglect the presence of a circumstellar disk. They describe the density distribution,  $\rho(r)$ , and the grain size distribution,  $n(a)$ , with power laws.

$$\rho(r) = \rho_o \left( \frac{R_{in}}{r} \right) \quad (4)$$

$$n(a) = A \left( \frac{a_{min}}{a} \right)^m \quad (5)$$

where  $\rho_o$  is the dust density at the inner edge of the dust shell,  $R_{in}$ , and  $a_{min}$  is the minimum dust grain size. They find that a combination of two populations of dust, a “hot” population at 1 - 11 AU, containing  $5.2 \times 10^{24}$  g ( $m = 2.8$ ) and a “cold” population at 28 - 175 AU, containing  $6.6 \times 10^{28}$  g ( $m = 2.0$ ), reproduces the observed 2-200  $\mu\text{m}$  *ISO* spectrum well. Their model fit parameters, including grain composition and the mass fraction of dust in each species, are reproduced in Table 4. Bouwman et al. (2000) assume that the iron oxide grains are small ( $2\pi a/\lambda \ll 1$ ) and do not infer a size distribution for this species.

Since Bouwman et al. (2000) do not predict the surface brightness of their model, we estimate the surface brightness of optically thin, spherically symmetric dust shells as a function of angular offset on the sky, assuming the same “hot” and “cold” populations of dust with the same power law dependences for  $\rho(r)$  and  $n(a)$  and the same composition. The specific intensity at an offset,  $b$ , from the star is calculated by integrating along the line of sight through the envelope, perpendicular to the sky.

$$I_\nu = \sum_{\text{all species}} \left[ \int_{x_{min}}^{x_{max}} \rho_i(r) \int_{a_{min,i}}^{a_{max,i}} B_\nu[T_{gr,i}(x)] n_i(a) Q_{abs,i} \pi a^2 da dx \right] \quad (6)$$

where  $r = \sqrt{b^2 + x^2}$  is the distance between the star and the dust grains whose radiation is summed in the integral. For the cold grains,  $x_{max} = \sqrt{175 \text{ AU}^2 - b^2}$  and  $x_{min} = 0$  for  $b < 28$  AU and  $x_{min} = \sqrt{28 \text{ AU}^2 - b^2}$  for  $b \geq 28$  AU. For the warm grains,  $x_{max} = \sqrt{11 \text{ AU}^2 - b^2}$  and  $x_{min} = 0$  for  $b < 1$  AU and  $x_{min} = \sqrt{1 \text{ AU}^2 - b^2}$  for  $b \geq 1$  AU. The grain temperature for each species,  $T_{gr}$ , is calculated

numerically, at a distance  $r$  from the star, assuming that the grains are in radiative equilibrium.

$$\left(\frac{R_*}{D}\right)^2 \int_0^\infty Q_{abs}(\nu) B_\nu(T_*) d\nu = 4 \int_0^\infty Q_{abs}(\nu) B_\nu(T_{gr}) d\nu \quad (7)$$

where  $T_*$  and  $R_*$  are the stellar radius and temperature,  $D$  is the distance between the star and the dust grain. We calculate the absorption coefficient for each species of dust,  $Q_{abs}(\nu)$ , and wavelengths less than  $0.2 \mu\text{m}$  following Bouwman et al. (2000). We calculate a total flux  $F_\nu(18.7 \mu\text{m}) = 45 \text{ Jy}$ , with 20 Jy produced by the hot population and 25 Jy produced by the cold population.

The Bouwman et al. (2000) model does not fit our data particularly well. After scaling the surface brightness to that of AB Aur, convolving a  $1.2'' \times 1.2''$  model of the dust emission with the PSF (MWC 480) yields a reduced  $\chi^2 = 8.6$ .

Bouwman et al. (2000) use grain materials which reproduce the *ISO 2 - 200  $\mu\text{m}$*  emission features well. They have some difficulty reproducing the observed near infrared visibilities. Their best fit model includes iron grains with radii  $0.01 - 0.1 \mu\text{m}$  to produce the near infrared emission close to the star. Iron is chosen as a material because it is one of the few materials which is likely to survive at temperatures  $\sim 1500 \text{ K}$  and its emissivity is high at near infrared wavelengths and low at mid- and far infrared wavelengths; there is no direct evidence for the presence of metallic iron from emission line features. The Bouwman et al. (2000) model is inconsistent with the measured visibility curves. A single grain population of metallic iron grains with radius,  $a = 0.32 \mu\text{m}$ , and minimum distance,  $R_{min} = 0.35 \text{ AU}$  fits the visibilities the best and reproduces the measured near infrared size of AB Aur. Bouwman et al. (2000) neglect the presence of a circumstellar disk altogether.

#### 4.3. A Flared Disk in Hydrostatic Equilibrium?

Another possibility is that the flat SED is produced by a flared disk. Flared disks intercept more stellar flux than geometrically flat disks, allowing surface grains to be warmed to higher temperatures. Flared disks have been observed around the young stellar objects HH 30 and HK Tau/c in scattered light using *HST* (Burrows et al. 1996; Stapelfeldt 1998). Simple semi-analytical models of flared disks with a layer of small ( $2\pi a/\lambda \ll 1$ ), optically thin, surface grains can reproduce the SEDs of some T Tauri and Herbig Ae stars (Chiang & Goldreich 1997; Chiang et al. 2001). Detailed numerical modeling has shown that stellar radiation is capable of heating the outer regions of the disk so that they become optically thin and vertically isothermal (D'Alessio et al. 1998). D'Alessio, Calvet, & Hartmann (2001) successfully model the SEDs and images of edge-on disks like HH30 and HK Tau/c.

D'Alessio et al. (2002) model the intensity of the dust around AB Aur at  $18.7 \mu\text{m}$  assuming that the central star has mass,  $M_* = 2.4 M_\odot$ , radius,  $R_* = 2.5 R_\odot$ , and effective temperature  $T_* = 9500 \text{ K}$  and is surrounded by a disk with inner radius,  $R_{min} = 3 R_*$  and an outer radius,  $R_{disk} = 200 \text{ AU}$ . They assume a disk inclination,  $i = 75.5^\circ$ , and a disk dust mass,  $M_{dust} = 5.6 \times 10^{29} \text{ g}$ , with a gas:dust ratio of 100:1. They assume that the disk is composed of silicates, trolite, ice, and organics with mass fractional abundances (relative to the gas mass) of 0.0034,

0.000768, 0.0056, and 0.0041 respectively (D'Alessio et al. 2001). The grains are assumed to have a size distribution described by a power law,

$$n(a) = Aa^{-3.5} \quad (8)$$

with a minimum grain radius,  $a_{min} = 0.005 \mu\text{m}$  and a maximum grain radius,  $a_{max} = 1 \text{ mm}$ . The assumption of grain growth in this model changes the opacity of the dust grains at small and large wavelengths and therefore the temperature distribution of the disk. Larger grain sizes decrease the fraction of stellar radiation intercepted by the disk resulting in a colder disk. The model assumes an accretion rate,  $\dot{M} = 1.0 \times 10^{-8} M_\odot/\text{year}$ , corresponding to an accretion luminosity of  $2 L_\odot$ .

The flared disk model does not fit our data particularly well. It predicts too little  $18.7 \mu\text{m}$  flux, 5 Jy, compared with all of the  $20 \mu\text{m}$  band flux measurements. This may partly be the result of the high assumed inclination,  $i = 75.5^\circ$ . Recent near infrared interferometry (Millan-Gabet et al. 1999) and scattered light imaging (Grady et al. 1999) suggests that the inclination of the AB Aur disk is probably less than  $45^\circ$ . Since the luminosity of the disk depends directly on the cosine of the inclination, the estimated flux of the D'Alessio disk might be as much as 2.8 times higher if it is calculated for an inclination of  $45^\circ$ . When the maximum surface brightness is scaled to that of AB Aur, convolving a model of the inner  $1.2'' \times 1.2''$ , with the most likely PSF (MWC 480) yields a reduced  $\chi^2 = 9.2$ . However, convolving the model with the worst PSF ( $\gamma \text{ And}$ ), yields a model which appears consistent with the observations.

The D'Alessio et al. (2002) model has some limitations. They assume a Pollack et al. (1994) grain mixture and ignore detailed grain composition information from infrared spectra. They do not fit the observed near infrared visibilities. However, their assumed circumstellar dust disk mass is an approximate agreement with that inferred from millimeter continuum measurements.

#### 4.4. A Flared Disk with a Hot Inner Rim?

The simplified flared disk model with a surface layer of small, optically thin grains predicts too little disk emission for AB Aur at near infrared wavelengths. Dullemond et al. (2001) have refined the Chiang & Goldreich (1997) flared disk model to allow for direct stellar heating of dust grains at the inner disk radius. In their model, grains sublime when their temperatures reach  $T_{rim} (= T_{sub} = 1500 \text{ K})$ . The direct stellar radiation on the inner rim surface warms the grains effectively, creating the observed near infrared excess, puffing up the inner disk, and casting a shadow on adjacent portions of the disk. Dullemond et al. (2001) model the AB Aur system with a star, with  $M_* = 2.4 M_\odot$ ,  $R_* = 2.5 R_\odot$ ,  $T_{eff} = 9520 \text{ K}$ , ( $L_* = 47 L_\odot$ ) surrounded by a disk with an inner rim  $R_{rim} = 0.52 \text{ AU}$  away from the star and an outer radius  $R_{disk} = 400 \text{ AU}$ . The vertical height of the inner rim is  $H_{rim} = 0.19 R_{rim}$ . In modeling the SED, the circumstellar disk is assumed to have an inclination,  $i = 65^\circ$ , less than that inferred from the CO observations of Mannings & Sargent (1997), more consistent with the  $45^\circ$  inclination inferred from scattered light observations of Grady et al. (1999). However, the model of intensity as a function of position was calculated

assuming that the AB Aur disk was face-on. Dullemond et al. (2001) assume a disk surface density

$$\Sigma = \Sigma_o \left( \frac{r}{1 \text{ AU}} \right)^{-2} \quad (9)$$

where  $\Sigma_o = 10^4 \text{ g/cm}^2$  with a total mass of  $4.0 \times 10^{29} \text{ g}$ . The gas:dust ratio is assumed to be 100:1. The dust grains are assumed to be a mixture of 95% astronomical silicate (Draine & Lee 1984) and 5% amorphous carbon (Ivezic et al. 1997). The rim and disk produce an  $18.7 \mu\text{m}$  flux,  $F_\nu(18.7 \mu\text{m}) = 49 \text{ Jy}$ .

The Dullemond et al. (2001) model does not agree with our mid-infrared observations. The reduced  $\chi^2$  for the model convolved with the PSF (MWC 480), in the inner  $1.2'' \times 1.2''$ , is 84, when the convolved image is scaled to have the same maximum surface brightness as AB Aur. Since the rim produces an order of magnitude less emission than the disk at  $18.7 \mu\text{m}$ , the Dullemond et al. (2001) model is essentially a Chiang & Goldreich (1997) flared disk with an inner radius of 8 AU. If the disk were to extend to an inner radius of 0.5 AU, 8% more  $18.7 \mu\text{m}$  emission would be produced (Dullemond et al. 2001) in the central pixel, only slightly affecting our normalization. Thus, the Chiang & Goldreich (1997) model similarly does not agree with our mid-infrared observations.

Dullemond et al. (2001) do fit other observational data well. They reproduce the measured near infrared fluxes and visibilities by placing the hot inner rim at the grain sublimation distance. Their assumed disk mass agrees with the dust mass, inferred from millimeter continuum measurements. They use a silicate/carbon grain mixture and do not match the infrared spectrum.

## 5. DISCUSSION

Models for the dust around AB Aur must fit a suite of multi wavelength observations if they are to be successful. In Table 5, we summarize the current ability of models to fit various observational data sets. In Table 6, we compare the predicted  $18.7 \mu\text{m}$  fluxes, dust disk masses, and reduced  $\chi^2$ s of each model to those inferred from observations. By examining the line cuts shown in Figures 4a and 4b, we see that the Dullemond et al. (2001) model

for the dust intensity predicts too much flux at distances  $\geq 0.24''$  (35 AU) from the star. If MWC 480 more accurately represents the PSF, then the Bouwman et al. (2000) model predicts too much emission and the D'Alessio (2002) model predicts too little emission at distances  $\geq 0.40''$  (58 AU) from the star. In this case, the Vinkovic et al. (2002) model is favoured. Flared disk models are not able to reproduce both the compact size of AB Aur and the strong mid-infrared flux. However, there is some uncertainty in the seeing at the time that AB Aur was observed; thus, it is not possible to rule out the flared disk model. Limitations exist with all the models, as described above. Future models of AB Aur must consider the grain composition, if they are to accurately model the SED and dust emission.

## 6. CONCLUSIONS

We have obtained high resolution mid-infrared images of AB Aur at  $11.7 \mu\text{m}$  and  $18.7 \mu\text{m}$  using the LWS on the Keck I telescope.

1. AB Aur is probably resolved at  $18.7 \mu\text{m}$ , with an angular diameter of  $1.2''$  at a surface brightness of  $3.5 \text{ Jy arcsec}^{-2}$ , and unresolved at  $11.7 \mu\text{m}$ , with a FWHM =  $0.30''$ .

2. Only  $\sim 10^{25} \text{ g}$  of dust is required to produce the  $18.7 \mu\text{m}$  emission. Millimeter interferometry indicates the presence of  $2 \times 10^{29} \text{ g}$  of dust. Thus, a large amount of cold dust must exist in the system, presumably in a disk.

3. The spatial distribution of the  $18.7 \mu\text{m}$  emission is most consistent with radiation from an optically thick, geometrically thin disk embedded in a spherically symmetric dust envelope (Vinkovic et al. 2002); however, the presence of a flared disk can not be excluded. None of the models yet reproduces all of the available observations.

This work has been supported by funding from NASA. We thank A. Sargent, B. Zuckerman, and our referee J. Bouwman for their comments. We also thank P. D'Alessio, C. Dullemond, and D. Vinkovic for providing us with models for the intensity of dust emission around AB Aur. P. Plavchan provided an IDL code to display the mid-infrared excess from AB Aur.

## REFERENCES

- Beskrovnyaya, N. G., Pogodin, M. A., Najdenov, I. D., & Romanyuk, I. I. 1995, *A&A*, 298, 585  
 Böhm, T., & Catala, C. 1993, *A&AS*, 101, 629  
 Böhm, T., & Catala, C. 1995, *A&A*, 301, 155  
 Bouwman, J., de Koter, A., van den Ancker, M. E., & Waters, L. B. F. M. 2000, *A&A*, 360, 213  
 Burrows, C. J., Stapelfeldt, K. R., Watson, A. M., Krist, J. E., Ballester, G. E., Clarke, J. T., Crisp, D., Gallagher, J. S. 1996, *ApJ*, 473, 437  
 Chiang, E. I., & Goldreich, P. 1997, *ApJ*, 490, 368  
 Chiang, E. I., Joungh, M. K., Creech-Eakman, M. J., Qi, C., Kessler, J. E., Blake, G. A., van Dishoeck, E. F. 2001, *ApJ*, 547, 1077  
 D'Alessio, P., Cantó, J., Calvet, N., & Lizano, S. 1998, *ApJ*, 500, 411  
 D'Alessio, P., Calvet, N., & Hartmann, L. 2001, *ApJ*, 553, 321  
 D'Alessio, P. 2002, personal communication  
 D'Antona, F., & Mazzitelli, I. 1994, *ApJS*, 90, 467  
 Draine, B., & Lee, H. M. 1984, *ApJ*, 285, 89  
 Dullemond, C. P., Dominik, C., & Natta, A. 2001, *ApJ*, 560, 957  
 Dullemond, C. 2002, personal communication  
 Gezari, D., Schmitz, M., & Mead, J. M. 1987, *Catalog of Infrared Observations Part II Appendixes (Greenbelt: NASA)*  
 Grady, C. A., Woodgate, B., Bruhweiler, F. C., Boggess, A., Plait, P., Lindler, D. J., Clampin, M., & Kalas, P. 1999, *ApJ*, 523, L151  
 Hillenbrand, L. A., Strom, S. E., Vrba, F. J., & Keene, J. 1992, *ApJ*, 397, 613  
 Ivezic, Z., Groenewegen, M. A. T., Menshchikov, A., & Szczerba, R. 1997, *MNRAS*, 291, 121  
 Jura, M., Ghez, A., White, R. J., McCarthy, D. W., Smith, R. C., & Martin, P. G. 1995, 445, 451  
 Mannings, V., & Sargent A. I. 1997, *ApJ*, 490, 792  
 Mannings, V., & Sargent A. I. 2001, *ApJ*, 529, 391  
 Marsh, K. A., Van Cleve, J. E., Mahoney, M. J., Hayward, T. L., & Houck, J. R. 1995, *ApJ*, 451, 777  
 Millan-Gabet, R., Schloerb, F. P., Traub, W. A., Malbet, F., Berger, J. P., & Bregman, J. D. 1999, *ApJ*, 513, L131  
 Millan-Gabet, R., Schloerb, F. P., & Traub, W. A. 2001, *ApJ*, 546, 358  
 Miroshnichenko, A., Ivezic, Z., Vinkovic, D., & Elitzur, M. 1999, *ApJ*, 520, L115  
 Natta A., Prusti, T., Neri, R., Wooden, D., Grinin, V. P., & Mannings, V. 2001, *A&A*, 371, 186  
 Ossenkopf, V., Henning, T., & Mathis, J. S. 1992, *A&A*, 261, 567  
 Palla, F., & Stahler, S. W. 1993, *ApJ*, 418, 414  
 Prusti, T., & Mitskevich, A. S. 1994, in *The Nature and Evolutionary Status of Herbig Ae/Be Stars*, eds. P. The, M. Perez, & P. van den Heuvel (San Francisco, Astronomical Society of the Pacific), 257

- Pollack, J. B., Hollenbach, D., Beckwith, S., Simonelli, D. P., Roush, T., Fong, W. 1994, ApJ, 421, 615  
 Richter, M. J., Jaffe, D. T., Blake, G. A., & Lacy, J. H. 2002, ApJ572, L161  
 Stapelfeldt, K. R., Krist, J. E., Menard, F., Bouvier, J., Padgett, D. L., Burrows, C. J. 1998, ApJ, 502, L65  
 Thi, W. F., van Dishoeck, E. F., Blake, G. A., van Zadelhoff, G. J., Horn, J., Becklin, E. E., Mannings, V., Sargent, A. I., van den Ancker, M. E., Natta, A., & Kessler, J. 2001, ApJ, 561, 1074  
 van den Ancker, M. E., de Winter, D., & Tjin A Djie, H. R. E. 1998, A&A, 330, 145  
 van den Ancker, M. E., Bouwman, J., Wesselius, P. R., Waters, L. B. F. M., Dougherty, S. M., & van Dishoeck, E. F. 2000, A&A, 357, 325  
 Vinkovic, D. Ivezic, Z., Miroshnichenko, A.S. & Elitzur, M. 2002, in preparation

TABLE 1  
 AB AUR PROPERTIES

Quantity	Adopted Value	Reference
Spectral Type	A0Ve+sh	1
Distance	144 pc	2
Effective Temperature ( $T_{eff}$ )	9500-10210 K	2, 5
Stellar Radius ( $R_*$ )	2.3-2.5 $R_\odot$	2, 5
Stellar Luminosity ( $L_*$ )	47-53.6 $L_\odot$	2, 5
Stellar Mass ( $M_*$ )	2.4-2.5 $M_\odot$	2, 5
Rotational Velocity ( $v \sin i$ )	80 km/sec	3
Fractional Dust Luminosity ( $L_{IR}/L_*$ )	0.44	4
Estimated Age	2-5 Myr	2, 5

References. — (1) Böhm & Catala (1993); (2) van den Ancker et al. (2000); (3) Böhm & Catala (1995); (4) Natta et al. (2001); (5) Mannings & Sargent (1997)

TABLE 2  
MEASURED 10  $\mu\text{M}$  FLUXES

Date Observed	Wavelength ( $\mu\text{m}$ )	Flux (Jy)	Reference
	10.1	25.2	Hillenbrand et al. (1992)
1993 Oct 23	11.7	20.6 $\pm$ 0.6	Marsh et al. (1995)
1994 Nov 14	11.7	23.0 $\pm$ 0.7	Marsh et al. (1995)
2000 Feb 20	11.7	25 $\pm$ 2	this paper
2000 Aug 9	11.7	19 $\pm$ 2	this paper
	12	30.4 $\pm$ 1.8	Prusti & Mitskevich (1994)
	12	23.8 $\pm$ 1.4	Prusti & Mitskevich (1994)
	12	18.7 $\pm$ 1.3	Richter et al. (2002)

TABLE 3  
MEASURED 20  $\mu\text{M}$  FLUXES

Date Observed	Wavelength ( $\mu\text{m}$ )	Flux (Jy)	Reference
	17	24.4	Thi et al. (2001)
	17	22.7 $\pm$ 2.3	Richter et al. (2002)
1994 Nov 14	17.9	34.7 $\pm$ 5.2	Marsh et al. (1995)
2000 Feb 20	18.7	31 $\pm$ 3	this paper
2000 Aug 9	18.7	17 $\pm$ 2	this paper
	20.25	27.2	Hillenbrand et al. (1992)
	25	49.6	Prusti & Mitskevich (1994)
	25	42.5	Prusti & Mitskevich (1994)

TABLE 4  
GRAIN PROPERTIES

Date Observed	Wavelength ( $\mu\text{m}$ )	Flux (Jy)	Reference	
Vinkovic et al. (2002):				
	$M_{frac}$	$a$ ( $\mu\text{m}$ )		
Astronomical Silicate	0.63	0.005-0.250		
Carbon	0.37	0.005-0.250		
Bouwman et al. (2000):				
	Hot $M_{frac}$	Hot $a$ ( $\mu\text{m}$ )	Cold $M_{frac}$	Cold $a$ ( $\mu\text{m}$ )
Olivine	0.71	0.01-5.0	0.74	0.01-126
Carbon	0.16	0.01-2.0	0.11	0.01-32
Water Ice	-	-	0.15	0.1-40.0
Iron	0.06	0.01-1.0	-	-
Iron Oxide	0.07	-	$9 \times 10^{-4}$	-
D'Alessio (2002):				
	$M_{frac}$	$a$ ( $\mu\text{m}$ )		
Silicate	0.25	0.005-1000		
Trolite	0.05	0.005-1000		
Ice	0.40	0.005-1000		
Organics	0.30	0.005-1000		
Dullemond et al. (2001):				
	$M_{frac}$	$a$ ( $\mu\text{m}$ )		
Astronomical Silicate	0.95	0.005-0.250		
Amorphous Carbon	0.05	0.16		

TABLE 5  
COMPARING THE MODELS WITH OBSERVATIONS

	Infrared Spectrum	18.7 $\mu\text{m}$ Image	Near infrared Visibilities
Vinkovic et al. (2002)	Omitted	Yes	Omitted
Bouwman et al. (2000)	Yes	No	No
D'Alessio (2002)	Omitted	Possibly	Omitted
Dullemond et al. (2001)	Omitted	No	Yes



TABLE 6  
MODEL PROPERTIES

	$F_\nu(18.7 \mu\text{m})$ (Jy)	Dust Mass (g)	Reduced $\chi^2$
Observed Quantities	31, 17	$2 \times 10^{29}$ †	
Predicted Quantities:			
Vinkovic et al. (2002)	25	$8.6 \times 10^{30}$	4.6
Bouwman et al. (2000)	45	$6.6 \times 10^{28}$ ‡	8.6
D'Alessio (2002)	5	$5.6 \times 10^{29}$	9.2
Dullemond et al. (2001)	49	$4.2 \times 10^{29}$	84

†Disk mass estimated from 2.7 mm interferometry (Mannings & Sargent 1997)

‡Dust in the Bouwman et al. (2000) model is located in spherically symmetric dust shells and not in a circumstellar disk.

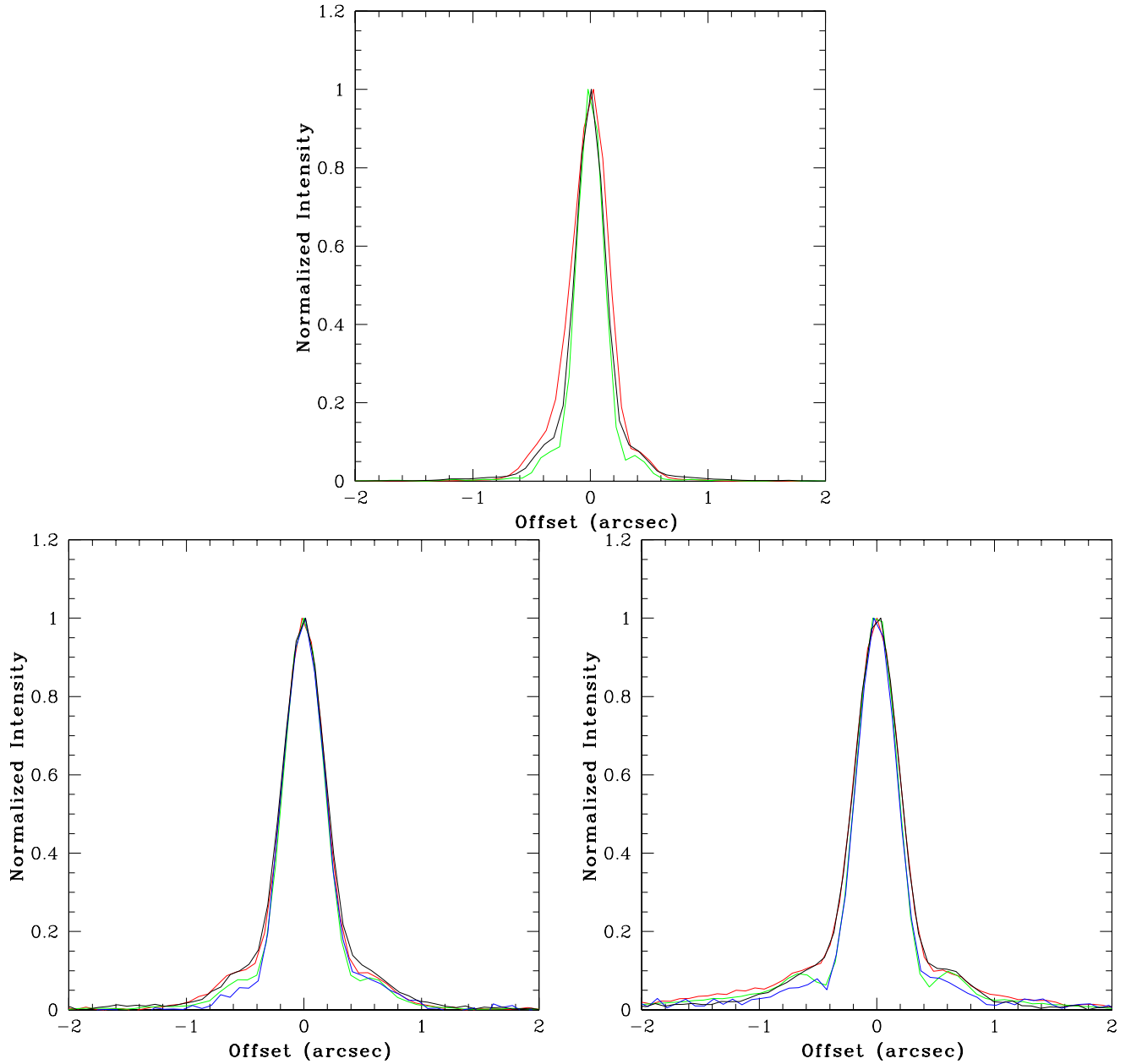


FIG. 1.— (a) Line cuts through AB Aur (black) and our  $11.7\ \mu\text{m}$  standard stars  $\gamma$  Dra (red) and  $\alpha$  Cet (green). (b) Line cuts through AB Aur and our  $18.7\ \mu\text{m}$  standard stars  $\gamma$  Dra (red),  $\alpha$  Cet (green), and MWC 480 (blue) made perpendicular to the direction of the asymmetric scattered light. (c) Line cuts through AB Aur and our  $18.7\ \mu\text{m}$  standard stars  $\gamma$  Dra (red),  $\alpha$  Cet (green), and MWC 480 (blue) made parallel to the direction of the asymmetric scattered light.

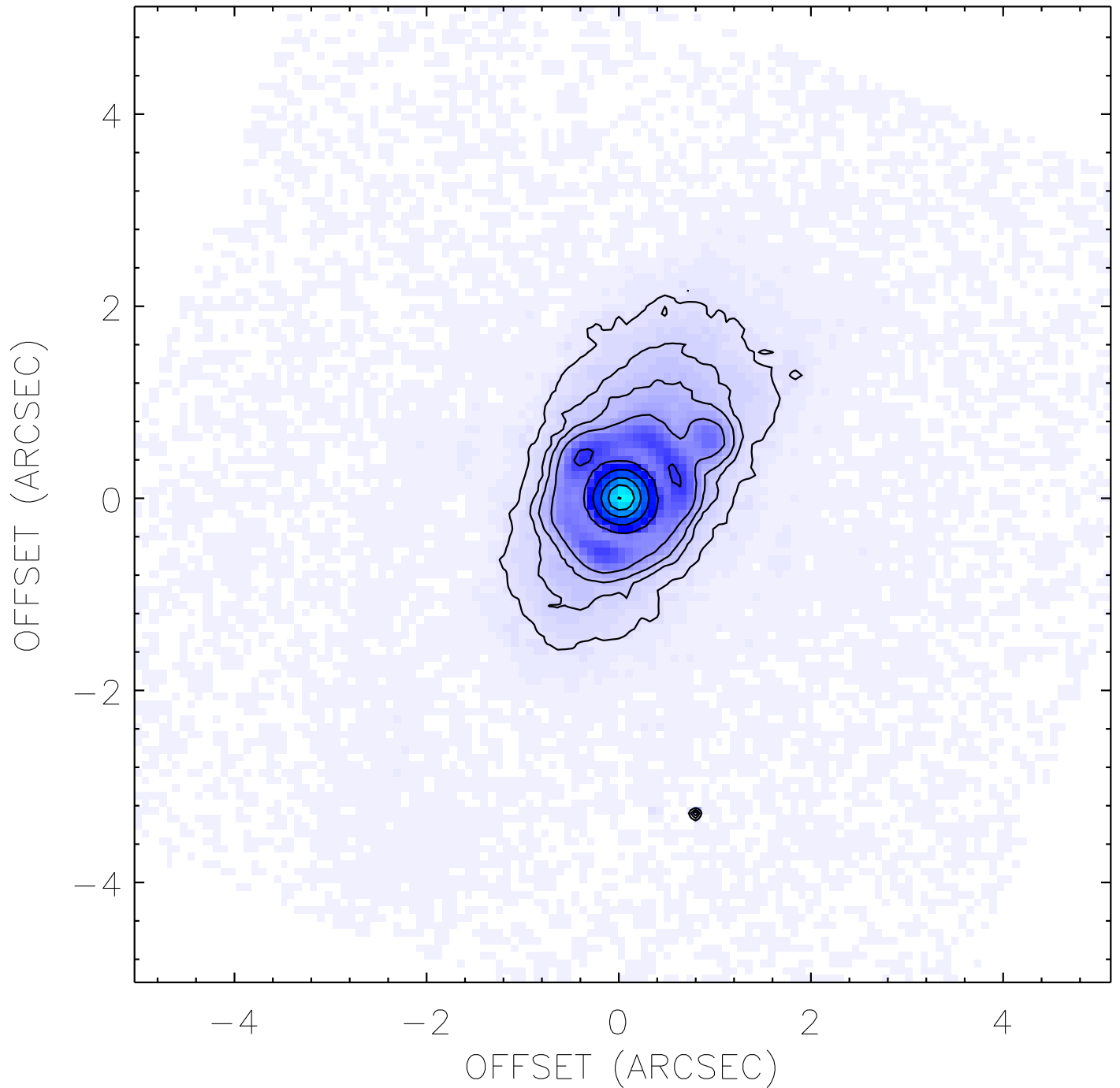


FIG. 2.— The  $18.7 \mu\text{m}$  image of  $\alpha$  Cet, our standard star, rotated so that the ghost appears in the same position as in the image of AB Aur. The contours show 1%, 2%, 3%, 5%, 10%, 25%, 50%, 75%, and 99% of the maximum surface brightness.

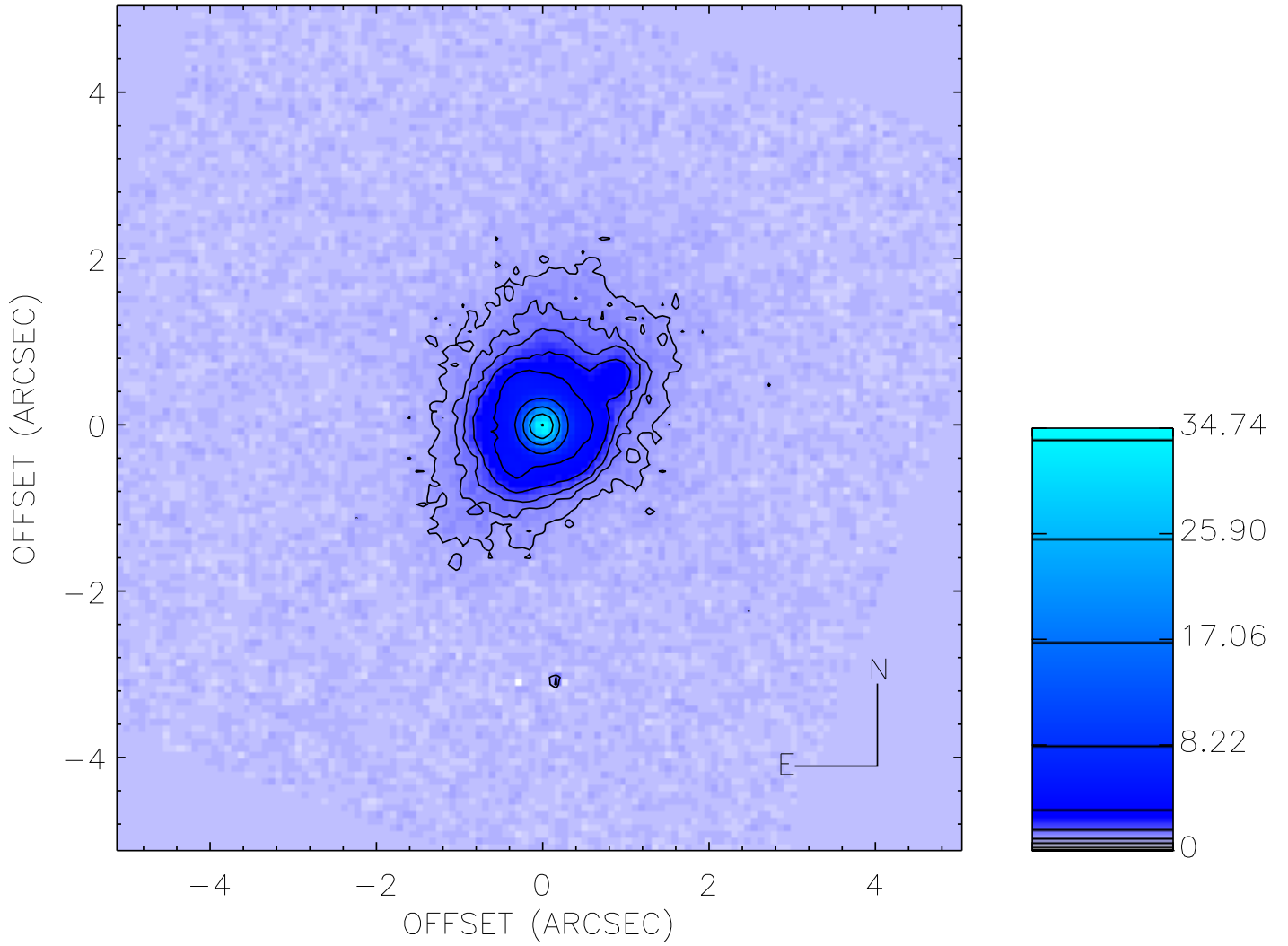


FIG. 3.— The 18.7  $\mu\text{m}$  image of AB Aur. North is up and East is to the left. The color bar shows the intensity key ( $\text{Jy arcsec}^{-2}$ ). The contours show 1%, 2%, 3%, 5%, 10%, 25%, 50%, 75%, and 99% of the maximum surface brightness.

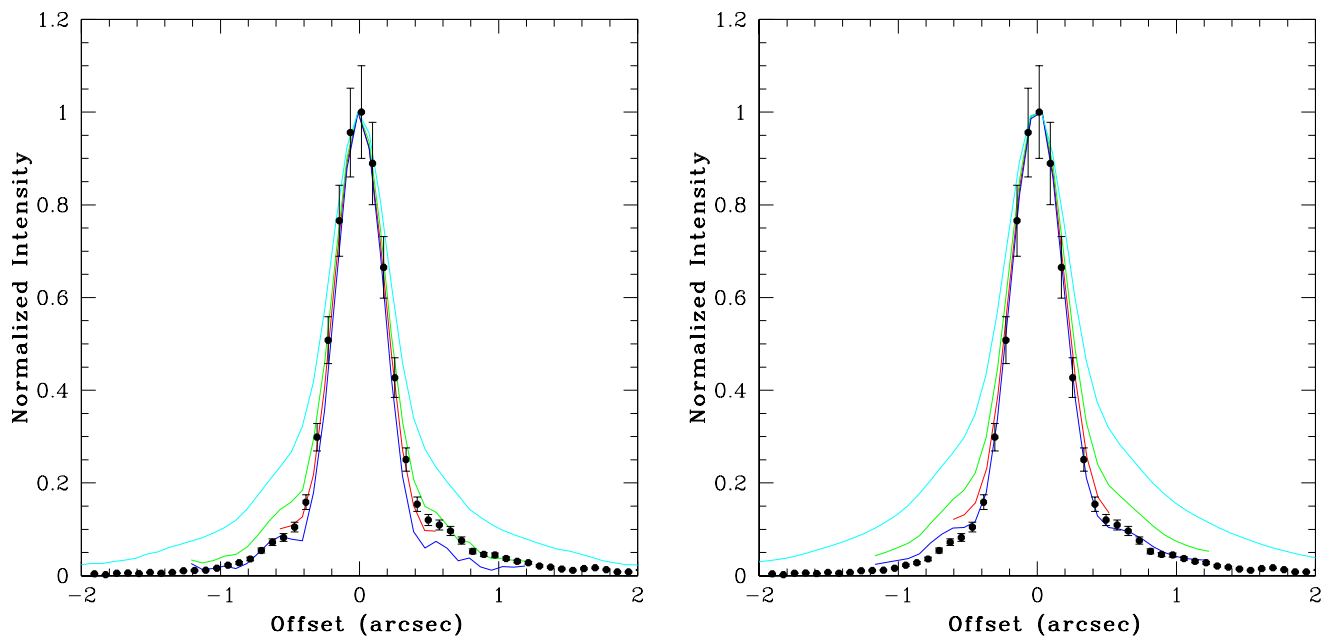


FIG. 4.— (a) Line cuts North-South through AB Aur at  $18.7 \mu\text{m}$  and each of the models convolved with MWC 480, the PSF observed closed in time to AB Aur. (b) Line cuts North-South through AB Aur at  $18.7 \mu\text{m}$  and each of the models convolved with  $\gamma$  Dra, the standard star observed with the worst seeing. The blue, red, green, and cyan lines (from bottom to top) show the D’Alessio (2002), Vinkovic et al. (2002), Bouwman et al. (2000), & Dullemond et al. (2001) models respectively.